Matrix Fluorescence Photobleaching Recovery for Polymer Molecular Weight Distributions and Other Applications

G. J. Doucet, D. Dorman, R. Cueto, D. Neau, and P. S. Russo*

Department of Chemistry and Macromolecular Studies Group, Louisiana State University, Baton Rouge, Louisiana 70803

D. De Kee

Department of Chemical Engineering, Tulane University, New Orleans, Louisiana 70118

J. Pople

Stanford Synchrotron Radiation Laboratory, Stanford Linear Accelerator Center, Stanford, California 94309

Received April 17, 2006; Revised Manuscript Received October 1, 2006

ABSTRACT: A new method for determining molecular weight distributions is explored. Matrix fluorescence photobleaching recovery (MFPR) requires dye attachment to the polymer analyte. No physical separation of macromolecules is accomplished, as in the predominant gel permeation chromatography technique. Rather, the distribution of diffusion coefficients is determined by inverse Laplace transformation of fluorescence photobleaching recovery decay profiles, and the diffusion data are then mapped onto molecular weight using a measured calibration. Resolution is enhanced by forcing the labeled polymer analyte to diffuse through a solution that contains unlabeled matrix, which can even be the same type of polymer. Relative to free diffusion, this increases the dependence of diffusion on molecular weight, making it easier to differentiate components having similar mass. Simulated, noise-corrupted data for molecules diffusing by reptation suggest that excellent resolution may be achieved. Empirical tests were conducted using fluorescent dextran and pullulan diffusers in unlabeled dextran matrix solutions. Although the resolution fell short of the simulated results, it exceeded that available from gel permeation chromatography as normally practiced. An investigation conducted to understand why the full resolution was not achieved revealed that matrix solutions of high molecular weight dextran lie in the unentangled semidilute regime, as evidenced by the scaling behavior of probe diffusion with probe molecular weight, the absence of a rheological plateau modulus, and the shape of the small-angle X-ray scattering profiles. Branching of high-molecular-weight dextran seems to preclude entry into the entangled regime, where a stronger diffusion vs mass relationship is expected. The good performance that was nevertheless achieved suggests that further exploration may prove fruitful.

Introduction

When gel permeation chromatography (GPC) was invented about 40 years ago,[1−9] the polymer analyst simply calibrated the molecular weight-elution volume profile with polymer standards, ran the samples of interest, and obtained a precise distribution of molar mass by mapping the output onto the calibration curve. GPC is only accurate when the standards are chemically identical to the unknown, but accuracy is often less important than precision and long-term reproducibility. Universal calibration schemes[10,11] remove much of the inaccuracy and are particularly effective with GPC/viscosity detectors.[12] The addition of light scattering detectors[13] (GPC/LS for a single scattering angle, GPC/MALS for multiple angles) removes almost all approximations and inaccuracies, at the expense of more required starting information (specific refractive index increment) and operational complexity, such as standardization to a Rayleigh reference, precise calibration of the concentration detector, normalization of the various scattering angles (GPC/MALS only), and interdetector time alignment.[14]

Probably no method for polymer characterization is more widely used than GPC in its various incarnations, but GPC-based measurement is not without problems. Run times are long, typically 15−45 min. Changing solvent, pH, salt, or temperature may require several hours. The expensive columns are easily damaged by dirty or reactive samples. A vast parts bin must be stocked for plumbing and maintenance of pump and detectors. Much solvent is consumed. Measurements can be made in aggressive solvents or at high temperatures, but only at the price of even more complexity and maintenance. The analyte should not adhere to the stationary phase, although this is less of a problem if a viscosity or light scattering detector is used. Finally, although good practice requires testing the column performance with frequent (regular GPC) or occasional (multidetector GPC) injection of calibration standards, nothing interesting is learned during this time-consuming activity. Elution volume lacks molecular significance.

An alternative to GPC was developed in the dynamic light scattering (DLS) community, partly motivated by the need to characterize polymers at very high temperatures or in aggressive solvents. A calibration curve of a different type is constructed by measuring diffusion coefficient (D) as a function of molecular weight (M). Unlike the elution volume vs molar mass calibration, this *is* molecularly interesting because the D vs M relationship provides an indication of molecular shape. The distribution of diffusion coefficients for the unknown is estimated by an inverse Laplace transform (ILT) algorithm[15,16] applied to the autocorrelation function, which takes the form

* To whom correspondence should be addressed. E-mail: chruss@lsu.edu.

10.1021/ma0608525 CCC: $33.50
Published on Web 12/07/2006

of a multiple-exponential decay. The distribution is then mapped onto the calibration curve to obtain the molar mass distribution. In this way, molecular weight distributions (MWDs) of very difficult-to-measure polymers have been estimated.[17,18]

The DLS/ILT approach might have found wider acceptance as a polymer characterization tool, were it not for poor resolution. The problem can be traced to the ill-conditioned nature of ILT for "noisy" data.[19] Even though DLS signal-to-noise ratios typically exceed 1000, it is difficult for ILT to resolve exponential decays separated by less than a factor of ~2. Diffusion usually follows a scaling law[20] with molecular weight, $D \sim M^{-\beta}$. An exponent of $\beta = {}^1/_2$ for an unperturbed chain implies that molar masses must differ by a factor of 4 to be resolved, which is unsatisfactory except for broad distributions. A way to improve the resolution is to force the polymer analyte to diffuse through a matrix polymer. This effectively stretches the D vs M behavior, raising β, because large polymers are more affected by the matrix than small ones. In the reptation limit,[20] $\beta = 2$, polymers differing in molecular weight by a factor of $\sqrt{2} \cong 1.4$ should be separable. This would be acceptable for many situations. Typical GPC installations may or may not perform any better, depending on column configuration. Even higher values of β have been reported.[21]

Many scattering experiments have been performed in a matrix solution for studies in polymer physics (see for example refs 22−28), and the sensitivity to molecular weight distribution has been noted.[29] Great care must be taken to match the refractive index of the matrix and solvent. Otherwise, the scattering from the matrix can dominate that from the polymer analyte. When index matching is imperfect, the results are not easily interpreted.[30,31] Even if the match is perfect, the matrix and polymer must be thermodynamically compatible to avoid aggregation or even outright phase separation. Finally, no one should relish the prospect of preparing dust-free analyte/matrix/solvent solutions.

The picture brightens considerably if the diffusion coefficients come not from DLS but from fluorescence photobleaching recovery (FPR).[32−34] In the matrix fluorescence photobleaching recovery (MFPR) experiments to be considered, the polymer to be analyzed is lightly tagged with a fluorescent molecule and dispersed at low concentration in a matrix polymer solution at much higher concentration. Neither dust nor the matrix polymer is detected. The matrix can be the same type of polymer as the analyte, lacking only the fluorescent tag, which neatly solves the compatibility issue (except in rare instances where a chain is incompatible with its own homologues across a molecular weight distribution). MFPR is similar in spirit to the original GPC because it relies on a calibration, but it is potentially much simpler and more robust. Thanks to the high sensitivity of fluorescence detection, a quantity of standard polymer sufficient to calibrate an MFPR instrument can be obtained by a *single* run of a broadly distributed sample on an analytical scale GPC/MALS followed by a fraction collector.[35] Other sample-efficient, absolute molecular weight methods, such as analytical ultracentrifugation, can also be used. Thereafter, these tools, which are more at home in a central research lab than in a production environment or, say, a space station, can be returned to physical studies and not be burdened with routine MWD analysis. Moving parts are not required in MFPR, changes in solvent, pH, and temperature are trivial, and mere microliters of solvent suffice. The need to label the analyte may seem to be a nuisance, but the chemistry of dye attachment has improved to the stage where it is often routine. The necessity of labeling can even be viewed as an opportunity because different ways to attach the dye—randomly along the chain or only at its end—can provide added flexibility.

In this paper, the potential of MFPR as a polymer analysis tool is first explored using simulated, noise-corrupted data. Success is measured in terms of the ability to resolve bimodal distributions. This is followed by an experimental test of the resolving power of MFPR using fluorescently labeled polysaccharides, either dextran or pullulan. Both are made to diffuse in a matrix of unlabeled, high molecular weight dextran. The results are interpreted with the aid of rheological and small-angle X-ray scattering measurements on the dextran matrix solutions and compared to some of the available theories for diffusion in polymer-containing solutions.

Background

Fluorescence Photobleaching Recovery. FPR methods have been reviewed recently.[36−42] In an ideal FPR measurement, some fraction of covalently attached dyes are destroyed without damaging the macromolecule or heating the solution. The recovery provides information about the diffusion. The original, simplest, and still most common form of the experiment, deep bleaching of a circular or Gaussian spot, is not well-suited to the problem at hand. Such spot photobleaching does not establish a simple boundary condition for the diffusion. Striped or fringed patterns are preferable, and several groups[32,43−45] have developed schemes that permit the diffusive recovery to be observed at a specific spatial frequency, K:

$$K = 2\pi/L \tag{1}$$

where L is the period of the pattern in the sample. To each diffuser, let us assign an index i and a fluorescent strength, F_i. At time $t = 0$, a photobleaching pulse is applied. The contrast, $C(t)$, of the striped or fringed pattern, which is typically proportional to a voltage output of the modulation detector system,[32,43,44] will fade according to a sum of exponential terms:

$$C(t) = B + \sum_i F_i e^{-D_i K^2 t} \cong B + \int_0^\infty F(\gamma) e^{-\gamma t}\, d\gamma \tag{2}$$

The baseline, B, represents noise from scratches on the cell or particulate matter in the sample, plus electronic jitter. In the integral form, which holds for the approximately continuous distributions of most synthetic polymers, a decay rate $\gamma = DK^2$ has been introduced.

The output of an ILT algorithm, such as the popular CONTIN program,[15,16] is a set of pairs of fluorescent amplitudes and decay rates, denoted by $[F,\gamma]$. Let index j represent an element, or grid point, of the set. The relationship connecting D and M may be written for each element of the set:

$$D_j = \frac{\gamma_j}{K^2} = \alpha M_j^{-\beta} \tag{3}$$

where the α is a prefactor. Molecular weight values for each grid point are obtained by inverting eq 2. Sometimes, in simple solutions, a distribution of hydrodynamic radius, R_h, is desired. This follows from the Stokes−Einstein law

$$R_{h,j} = \frac{kT}{6\pi\eta D_j} \tag{4}$$

where k is Boltzmann's constant, T the Kelvin temperature, and η the solvent viscosity.

The relationship between fluorescence strength and polymer concentration depends on the labeling scheme. Adopting most of the notation from ref 46, we may write

$$F_j \propto pN_jM_j^{\delta} = p'N_jR_{h,j}^{\sigma} \quad (5)$$

where N_j is the number of diffusers associated with the jth grid point. The coefficients p and p' formally account for variation in labeling efficiency and quantum yield with mass and size, respectively; here, they will be treated as constants. The parameters δ and σ reflect the nature of the dye attachment. The fluorescence intensity does not depend on mass or size for end labeling of linear polymer chains (or any other scheme that puts exactly the same number of dye moieties on each diffuser). In such cases, $\delta = \sigma = 0$, and the fluorescence intensity is proportional only to the number of diffusers. Labeling of a polymer chain randomly along its length corresponds to $\delta = 1$, while σ depends on the architecture of the chain (e.g., $\sigma = 2$ for a Gaussian random coil). Now the fluorescence intensity is proportional to the number of diffusers multiplied by their molecular weight, i.e., to the total mass or mass density, c (e.g., g/mL). Equations for solid spheres were given earlier.[46] The ability to control how intensity depends on size provides additional power not available to DLS. That technique always sees an amplitude proportional to $N_jM_j^2$, veiled at finite angles by a particle form factor that depends on shape. If the shape is not known, or not uniform across the distribution, the experiments must be conducted at low angles where interference from dust is strongest and signal acquisition longest. In FPR, one may be able to choose end labeling to ensure that small polymers can be seen in the presence of large ones. Even with random labeling, FPR detects the first moment of the distribution, while DLS senses the second.

Equations 3−5 show that it is a simple matter to convert $[F,\gamma]$ to $[N,M]$, but how well might we be able to determine $[F,\gamma]$ in the first place? A good way to find out is to simulate bimodal distributions according to $D = \alpha M^{-\beta}$, add realistic levels of noise, and test whether CONTIN can resolve the two peaks. Extensive comparisons of CONTIN and other methods (see, for example, ref 47) suggest that CONTIN is representative of the better algorithms. As the focus here is to evaluate the potential of a new experiment that may offer inherently greater resolution, other ILT choices are not considered.

Polysaccharide Solution Behavior. Dextran is a polysaccharide produced by the *Leuconostoc mesenteroides* bacterium, strain B-512(F). The molecules are composed of α-D-glucopyronosyl residues primarily linked at the α(1−6) position.[48] Dextran is considered to belong to the class of branched molecules. Branching occurs when (1−2), (1−3), or (1−4) links appear along the backbone. Short chain branching accounts for about 5% of the links even though branching density as high as 30% has been reported.[48−55] Long-chain branching is observed in molecules with a molecular weight of 150 000 Da. Pullulan is a polysaccharide produced by the *Aureobasidium pullulan* fungus as a linear polymer consisting of maltotriose repeat units linked at the (1−6) position by a glycosidic bond.

Although many studies have used dextran and related polymers as dilute probes of various environments (see, for example, ref 56), only recently have there appeared detailed studies of concentrated solutions, which address the nature of overlap in these branched polymers.[51] Diffusion of small solutes and larger micelles in concentrated dextran in solution and gel form has been studied, though.[57,58] It was found[57] that specific interactions did not play a strong role in diffusion, suggesting the importance of physical impediments. Many theories have addressed this problem,[59−69] and the detailed nature of the constraints is beginning to be worked out experimentally by varying the molecular architecture of probe and matrix.[70]

Experimental Section

Fluorescence Photobleaching Recovery System. The apparatus follows the prescription of Lanni and Ware,[32,33] except that the striped illumination pattern (Ronchi ruling) is now wiggled instead of translated over long distances. The electromechanical modulation detection system initially reports a triangle-shaped signal at the photomultiplier tube. This quickly rounds to a sine wave as terms associated with high spatial frequencies fade. The signal amplitude at the fundamental frequency (typically 32 Hz) is detected by a peak voltage detector triggered by a zero crossing circuit. The number of points detected is large. While many experimental methods in various fields of science rely on multiple exponential decays, DLS practitioners were the first to discover that the entire record (linearly spaced correlation function, in their case) is not necessary; for maximum efficiency, data along the time axis should be grouped logarithmically.[71−74] Modern correlators for DLS often use a quasi-logarithmic scheme, with blocks of lag time channels separated by equal increments, each block rising up by a power of 2. A similar "blocking" routine is applied to our FPR record, either real or simulated, meaning that data gathered long after the photobleaching pulse are averaged over longer times and, therefore, quieter than data from the early part of the recovery. The noise profile qualitatively resembles that of DLS performed with a modern, logarithmically spaced correlator. Further details of the apparatus appear in the Supporting Information.

Inverse Laplace Transformations. The MFPR distributions (apparent chromatograms) that appear below are an average of three normalized results from three different measurements. The error bars for amplitudes are the standard deviations. Averaging of "chromatograms" is possible because the range of decay rates in CONTIN and the number of points between the minimum and maximum decay rates was kept constant. Scaling of the "chromatograms" was accomplished by dividing the amplitude associated with each decay value by the sum of all amplitudes then multiplying by an arbitrary number so details can be seen.

Simulation of FPR Recoveries. Recovery curves were simulated using a software package that was developed to support the FPR apparatus. The simulation is designed to match the normal output of the FPR instrument. The program also combines a cumulants-style linear polynomial fit, multiple-exponential nonlinear fit and CONTIN Laplace inversion into an intuitive, graphical interface. The ability to simulate multiple exponential decays should be part of any ILT package because the ill-posed nature of ILT often leads to questions like, "can this apparent separation be real"? The user answers such questions by simulating the distribution, adding noise comparable to that present in the experiment, and testing.

In the simulations, we assigned a diffusion of $D = 2.0 \times 10^{-7}$cm^2 s^{-1} to $M = 10\,000$, scaled the diffusion at other molecular weights according to the reptation prediction of $D \sim M^{-2}$, and applied 3% noise to the unblocked data. The spatial frequencies selected for the simulations correspond to the use of an epi-illumination FPR microscope with 10× objective to cast into the sample the image of a Ronchi ruling having either 50 or 100 lines/in. Under these conditions, data acquisition times (and simulated recovery times) are typically ∼20 min, which is similar to GPC with two columns. The CONTIN parameters were set to span a wide range of decay times with 50 grid points. They were not optimized from run to run to test simple, "push-the-button" operation. CONTIN produces many trial solutions and automatically selects one to be the smoothest distribution consistent with the data. This solution was used, except as noted.

Gel Permeation Chromatography. The aqueous GPC used to characterize dextran and pullulan samples was assembled from a Waters Associates chromatography pump model 6000A, a Polymer Labs Aquagel chromatography column part number 1149-6800, a Wyatt Technology Corp. Dawn DSP laser photometer operating at

Table 1. Characterization of Fluorescein-Labeled (FD) Dextran Probes and Dextran Matrix[a]

sample	lot no.	vendor's M/1000	GPC-MALLS M_w/1000	GPC-MALLS PDI	R_h/nm	R_h/nm from ref 15
FD4	38H-1768	4.4	5.0 ± 0.2	1.15 ± 0.01	1.4	1.3
FD10s	38H-5083	9.5	11.2 ± 0.3	1.18 ± 0.01	2.3	1.7
FD20	77H-0361	21.2	27.4 ± 0.4	1.36 ± 0.02	3.3	2.8
FD40	39H-0871	38.2	42.4 ± 0.9	1.22 ± 0.02	4.5	4.5
FD70	117H-0564	71.6	80.6 ± 0.5	1.19 ± 0.01	6.0	5.8
FD150	127H-5080	148	161 ± 4	1.84 ± 0.02	8.5	8.8
FD500s	38H-5082	500	456 ± 8	1.96 ± 0.02	unknown	13.3
matrix	98H-0939	2000	4150 ± 261	3.21 ± 0.28	27.0	unknown

[a] The samples are listed by the Sigma-Aldrich catalog number. R_h is calculated from D^0 measured in FPR.

Table 2. Characterization of Pullulan Probes before and after Labeling[a]

	unlabeled			labeled		
sample	M from Polymer Labs/1000	GPC-MALLS M_w/1000	GPC-MALLS PDI	GPC-MALLSM_w/1000	GPC-MALLS PDI	R_h/nm
pullulan	11.8	11.5 ± 0.2	1.33 ± 0.04	22.4 ± 8.5	1.61 ± 0.50	2.3
	22.8	29.3 ± 12.5	1.62 ± 0.15	26.1 ± 0.6	1.67 ± 0.17	3.3
	47.3	50.1 ± 5.2	1.36 ± 0.04	48.6 ± 14.9	1.75 ± 0.40	4.1
	100.0	109.8 ± 7.6	1.58 ± 0.19	104.2 ± 8.7	1.43 ± 0.04	7.5
	380.0	408 ± 16.5	1.63 ± 0.26	393.8 ± 15.3	1.65 ± 0.14	14.3

[a] R_h for the labeled pullulan is calculated from D^0 measured in FPR.

632.8 nm, and a Waters Associates differential refractometer model R401. The Dawn was calibrated using toluene as the Rayleigh reference, and the multiple detectors were normalized using low-M pullulan standards from Polysciences, Inc. The mobile phase for all experiments on the GPC-MALS was a sodium phosphate buffer[75] of pH = 7.8 with 5.0 μM sodium azide made with water from a Barnstead Nanopure filtration system. Typical concentrations for injected samples range from 1 to 5 mg/mL. Samples were run in triplicate for the measurement of number-average molecular weight, M_n, weight-average molecular weight, M_w, and polydispersity index, PDI = M_w/M_n. Separation of dextran and pullulan mixtures was attempted with the same setup after substituting a series of columns specifically selected for good performance in the desired range (Polymer Laboratories Aquagel-OH: 40A, molecular weight range 10 000−200 000; 50A, molecular weight range 50 000−1 000 000).

Rheology. A Rheometrics Scientific SR5000 controlled stress rheometer with a parallel plate setup was used to measure the storage modulus, G', and viscosity, η, of the matrix solutions. Measurements of G' were done using oscillating shear, varying the frequency at constant strain. The range of frequencies used to measure G' was 1 to 100 s^{-1} with 10 points for each decade. The stress for dextran matrix solutions with w = 0.25, 0.20, 0.15, 0.10, and 0.05 was 100, 75, 50, 20, and 10 Pa, respectively. Viscosity was measured using the torque during a constant shear experiment. Storage modulus results are reported over the range of frequencies. Each solution of a given weight fraction was measured in triplicate at identical frequencies so the storage modulus and viscosity measured at one particular frequency could be averaged.

Small-Angle X-ray Scattering. Small-angle X-ray scattering (SAXS) data were obtained at the Stanford Synchrotron Radiation Lab, SSRL, at beamline I-4. Five samples with concentrations representative of those used for the diffusion calibration plots were measured. The scattering data were collected with λ = 0.1488 nm. The liquids cell, designed and built at SSRL, sandwiches the fluid between polyimide film, with an average path length of 1 mm.

Dextran. The dextran used for matrix solutions was purchased from Sigma (Catalog # D-5376 Lot # 98H-0939, average M = 2 000 000 Da). Fluorescein isothiocyanate, FITC, and labeled dextrans (FD) were used as received from Sigma. The molecular weights of the probes and matrix dextrans were characterized using GPC-MALS, and the results are found in Table 1. The molecular weights measured by GPC-MALS either agree with or slightly exceed the vendor-supplied values.

Pullulan. Fluorescently labeled pullulan probes (FP) were prepared from a set of GPC standards from Polymer Laboratories, Cat. # 2090-0100, and 5-(4,6-dichlorotriazinyl)aminofluorescein (5-DTAF) from Molecular Probes. Pullulan was dissolved at a concentration of 10 mg mL^{-1} in sodium hydroxide, pH 10, and likewise for 5-DTAF at a concentration of three dye molecules per pullulan molecule. The reaction mixture was stirred for 28 h at room temperature, and then 1 M hydrochloric acid was added while monitoring with indicating paper until pH = 7.0−7.2 was reached. Millipore Ultrafree-4 centrifugal filter units (Cat. # UFVBGC25) were used to remove excess 5-DTAF from the samples. The 5-DTAF-labeled pullulan was freeze-dried to remove any excess solvent. Pullulans before and after labeling were characterized using GPC-MALS. The results appear in Table 2. The molecular weights and polydispersity values measured could be skewed due to a change in the dn/dc value from attaching the 5-DTAF and peak broadening, but due to the light labeling this seems unlikely.

Solutions. Matrix solutions were prepared by adding 5 mM NaN_3 solution to the matrix dextran for the desired concentration and were inverted each day 25 times until dissolved. The sodium azide solution was prepared from NaN_3 (J.T. Baker Chemical Co.) and water (Barnstead Nanopure deionization system series 630). Calibration samples were prepared by placing a small amount FD or FP (<0.01 mg) into a 2.5 mL vial. The matrix solution was then added on top of the solid, filling approximately three-quarters of the vial, ensuring a negligible change in total concentration. Vials containing the probe/matrix solutions were rotated at a slow speed around their long axes by a homemade spinning device for a week and were inverted 25 times each day. Samples to be used for the resolution tests were prepared by pipetting two or three different dilute solutions of labeled dextran or labeled pullulan into a vial and then dried using a vacuum oven. The amount of the solution was regulated to produce the desired ratio of fluorescence in the sample. The matrix of choice was added to the dried probe molecules and mixed for 3 days.

Results and Discussion

Ease of Labeling. Many if not most water-soluble polymers are easily labeled, the pullulan here being typical of polysaccharides. The time required for labeling is not an important limitation because good practice for most other methods requires extensive dissolution that requires preplanning anyway. As a challenge, we attempted to measure the diffusion profile of a polymer unknown by FPR and by DOSY NMR. A day was chosen when the NMR was available, ensuring that the results from NMR came first; however, the gradient specifications were poorly optimized. (DLS practitioners of a certain age will remember the importance of establishing the sample time; DOSY NMR still has this limitation, there being no equivalent

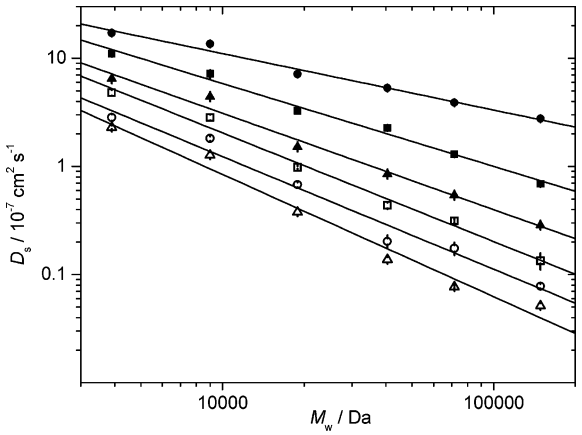

Figure 1. Diffusion of fluorescently tagged dextran in unlabeled dextran matrix of $M_w = 2\,000\,000$ Da: no matrix (●), 5% w/w matrix (■), 10% w/w matrix (▲), 15% w/w matrix (□), 20% w/w matrix (○), and 25% w/w (△).

of the modern autocorrelator that spans 11 decades of time, or even of FPR as practiced here, which spans 2−4 decades depending on user patience.) By the time an appropriate gradient matrix was devised, the sample had been labeled, isolated from unreacted dye, and successfully measured by FPR. It is not difficult to imagine that labeling could be automated. In an age when minute fragments of DNA are automatically amplified to measurable levels, there is no reason to fret over dye chemistry, especially of water-soluble polymers.

Simulations. The ability to resolve two peaks from noise-corrupted FPR data was consistent with what has been known about CONTIN for some time: for typical levels of noise, it is possible to resolve two peaks when their decay rates differ by about a factor of 2 or more. Signals corresponding to polymers with molecular weights 10 000 and 20 000 were separable when $\beta = 2$, but not when $\beta = {}^1/_2$. An important parameter is the minimum polydispersion index that might be believed for a perfectly sharp peak, which was about 1.05 for the CONTIN-chosen solution. This is not a practical problem for all but very detailed characterizations. More about the simulations appears in the Supporting Information, where it is evident that many polymer distributions could be characterized by MFPR when $\beta = 2$.

Scaling Relations. The scaling exponent for labeled dextran in water was found to be $\beta = 0.52 \pm 0.03$ (Figure 1), which is typical of random coil polymers in dilute solution.[20] Furukawa and Ware[49] measured the infinite dilution values, $D°$, for fluorescein and two different molar masses of dextran in dilute solution, obtaining $\beta = 0.52 \pm 0.01$. Bu and Russo[76] measured the diffusion of labeled dextran through the matrix of hydroxypropyl cellulose (HPC); β in dilute solutions of dextran in the absence of HPC was 0.53 ± 0.02 for molecular weights in the range of this study. When two higher-M samples from that study are included, β becomes 0.44 ± 0.03, probably due to structural effects (branching) not present in the samples at lower M. Ioan et al.[48] report $\beta \sim 0.45$. As matrix is added β climbs, reaching $\sim$1 at the highest weight fraction, w. This resembles Rouse-like behavior.[77] There is no evidence for entanglement because β never reaches the reptation expectation[20,78] of 2, let alone the empirical value, 2.3 ± 0.1,[79−81] which may be understood in terms of extensions to the original reptation theory.[82]

As shown in Figure 2, similar results were achieved for the pullulans: $\beta \sim 0.5$ in dilute solution, and $\beta \sim 1$ as the dextran matrix concentration rises. Again there is no sign of entanglement. Matrix weight fractions did not exceed $w = 0.15$ because

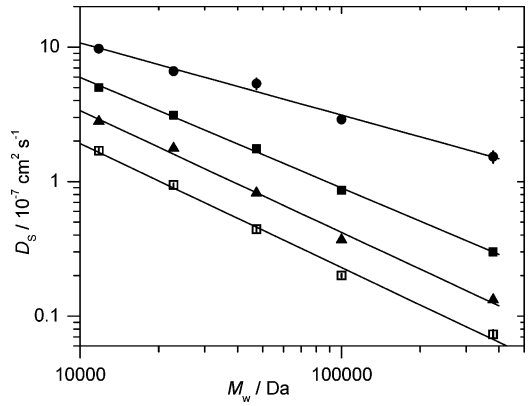

Figure 2. Fluorescently tagged pullulans diffusing through dextran matrices: no matrix (●), 5% w/w (■), 10% w/w (▲), 15% w/w (□).

no significant improvements were anticipated, given the behavior of the dextran probes. Even though β does not reach the reptation limit, the reasons for which are considered below, the results suggest that added matrix will improve the ability of FPR to resolve bimodal polymer solutions.

Resolution Tests. Several bimodal systems were studied.[83] When the separation in molar mass was large, the expected bimodal character was evident even without added matrix, but polydispersity indices for the individual peaks were overestimated. This is a consequence of the natural "line broadening" of ILT (as the grid points of the algorithm are finite in number and not guaranteed to match a single, sharp decay rate arising from a monodisperse sample, several adjacent grid points may be assigned finite amplitude). Addition of 5% matrix sharpened the peaks, as shown in Figure 3 for a 1:3 mixture (by fluorescent intensity) of 11.8 and 380 kD fluorescent pullulan.

This is the expected consequence of the "stretching" of the D vs M relationship (rise in β). Molar mass accuracy was within about 15% but worsened as matrix was added. Relative concentrations were estimated well ($\sim$3% error). Studies of a reverse mixture (i.e., 3:1 11.8 and 380 kD FP) again showed the sharpening of the individual peaks as matrix was added, but molar mass accuracy of the heavy component was reduced, as was that of the relative concentrations. It is difficult to imagine a dilute solution DLS experiment that would better these results; the weak scattering from the 11.8 kD component would be difficult to detect in the presence of the 380 kD material. The often quieter signal from DOSY NMR might prove superior, assuming the availability of an NMR-invisible, yet thermodynamically compatible, matrix. These 11.8 kD/380 kD mixtures would be easily resolved by GPC. The potential of MFPR becomes more readily apparent when closely spaced bimodal samples are tested.

As shown in Figure 4, complete inability to detect the presence of FD20 and FD70 in dilute solution improves to the appearance of a definite shoulder when matrix is added. This is hardly baseline resolution, but it is encouraging. To this point, ILTs have been conducted in automatic, "push-the-button" mode because of our eventual interest in a simple method for technicians with little training. Thus, the number and location of CONTIN grid points was set to cover a very broad range of molecular weights and left unaltered. Only the solutions chosen by the program have been shown. Better use of CONTIN requires "squeezing" the grid points (by varying the first and last decay rates considered) to match the actively decaying part of the curve and full consideration of all the distributions proposed by the program (which vary according to the strength of the regularizer) in terms of their residuals, including

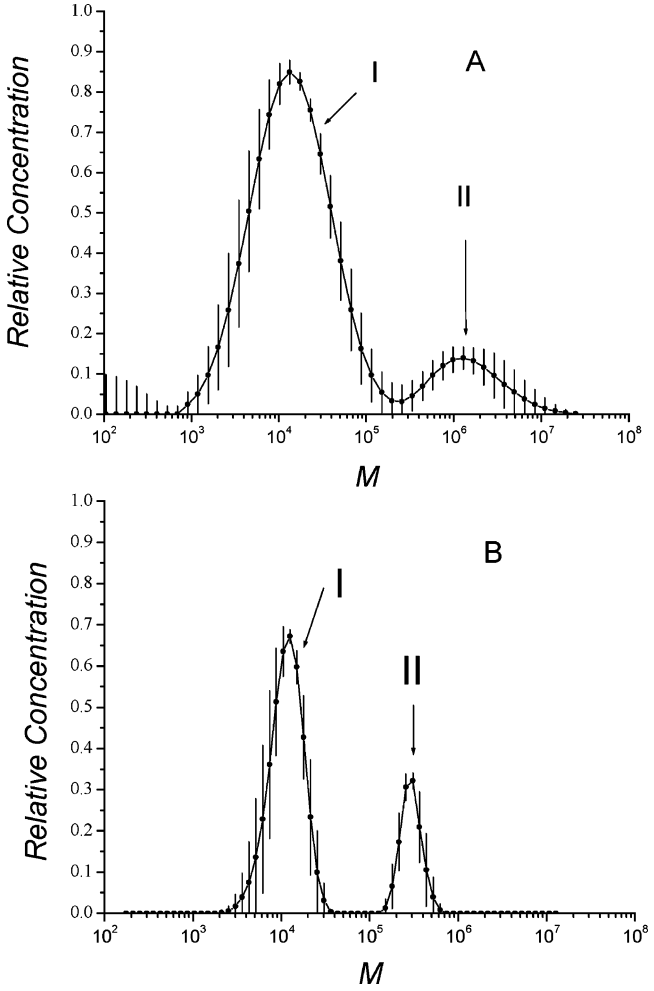

Figure 3. CONTIN results from FP380:FP11.8 mixtures in a 1:3 ratio diffusing through different dextran matrices: (A) no matrix; (B) 5%.

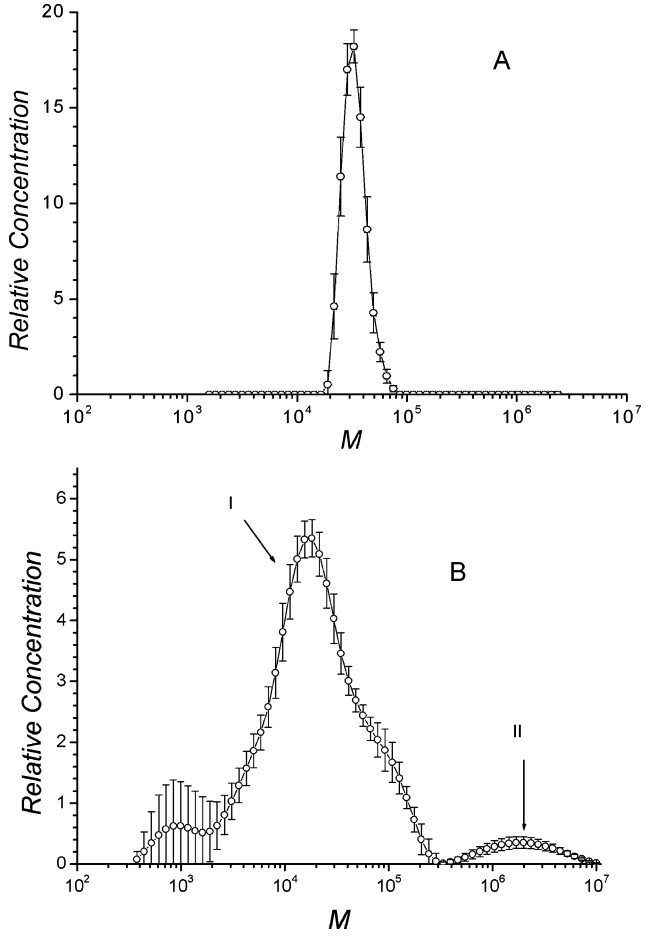

Figure 4. Detecting FD20 and FD70 dissolved in dextran matrix solutions. Concentrations of the matrix solutions are (A) no matrix and (B) 10% w/w.

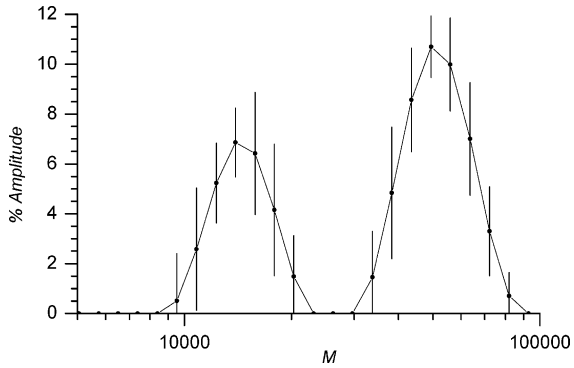

Figure 5. Representative distributions calculated by CONTIN and chosen by the user showing the detection of FD20 and FD70 in a mixture. The weight percent of the matrix solutions was 0.25. Spurious peaks at low and high *M* not shown.

systematic trends. In Figure 5, a satisfactory resolution of FD20 and FD70 is displayed, in this case at a matrix content of $w = 0.25$. The error bars represent repeat measurements. The bimodality was evident at other matrix contents, too.

One may ask how GPC/MALS would perform when it comes to separating these same two dextrans; this is discussed in the Supporting Information. Briefly, we agree with others[48] that the resolution of closely spaced dextrans is not such a simple matter as often supposed. From the standpoint of resolution of dextrans, MFPR certainly seems competitive with GPC as it is normally practiced, even when the scaling exponent has only risen to $\beta \sim 1$.

As an alternative to ILT, and as noted previously,[76] one may choose a simple multiexponential analysis. The results appearing in Table 3 suggest that the matrix does greatly help FPR find the correct amplitudes (50% for each component). Even at relatively low matrix concentrations, the two-exponential (2EXP) analysis returns reasonable molecular weights.

Physical Characterization of Aqueous Dextran as a Polymer Matrix Material. The low β values seen here and elsewhere[51,81,84−87] suggest that the matrix polymer, despite its high molar mass, did not become self-entangled and therefore was not fully capable of restraining the diffusion of the larger probe molecules. Only in recent years have very detailed studies of dextran solutions at high concentrations appeared.[51] In what follows, we attempt to further the understanding of concentrated dextran solutions in molecular terms.

As noted already, dextran is described as a branched molecule when M exceeds 150 000 Da.[51,88,89] Branches of short and intermediate length may interfere with entanglement because the molecular interiors crowd upon themselves, never interpenetrating. GPC/MALS measurements of the fluorescein-labeled dextrans reveal a relationship, $R_g \sim M^{\nu}$ with $\nu \approx 0.41$, for FD150 and FD500s. (See Supporting Information, where only R_g values exceeding about 10 nm were used, this being about 1/45th the laser wavelength in solution; likewise, data for molecular weights of FD70 and FD40 are shown in the Supporting Information but not included in the analysis.) This exponent is reasonable, given the result of ref 76 that $D \sim M^{-0.44\pm0.03}$ when high-M dextran data are included, because D

Table 3. Results from One-Exponential (1EXP) Analysis (No Matrix) and Two-Exponential (2EXP) Analysis (Otherwise) of FPR Measured Decay Curves of Mixtures of FD20 and FD70 in Different Matrices[a]

matrix wt %	M_1/1000	% M_1	M_2/1000	% M_2
no matrix	32 ± 7	N/A	N/A	N/A
5	21 ± 3	80.5 ± 1.9	170 ± 24	19.5 ± 1.9
10	14 ± 2	71.0 ± 6.3	94 ± 13	29.0 ± 6.3
15	16 ± 2	59.3 ± 8.9	67 ± 7	40.7 ± 8.9
20	23 ± 4	66.1 ± 4.3	92 ± 15	33.9 ± 4.3
25	16 ± 3	51.1 ± 2.1	56 ± 8	48.9 ± 2.1

[a] M_1 and M_2 relate to the fast and slow diffusion components. The percentages indicate the amount each contributes to the decay and thus the relative concentration.

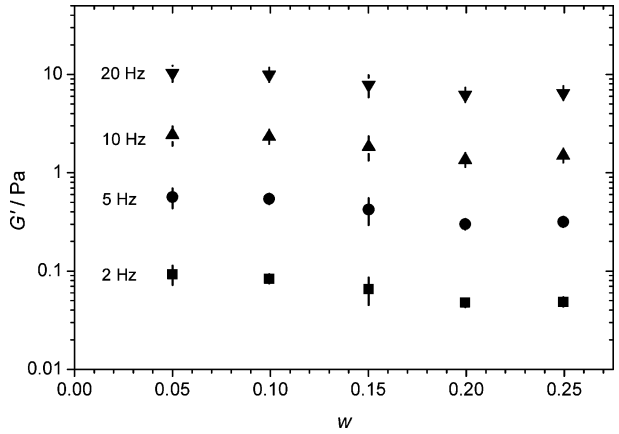

Figure 6. Illustration of the change of G' over the range of dextran matrix concentrations at oscillation frequencies 2 (■), 5 (●), 10 (▲), and 20 Hz (▼).

$\sim R_h^{-1}$ and R_h is proportional to R_g as a first approximation. (The dynamic scaling exponent is slightly less than the static,[94] reinforcing the case for a low β value.) The expected results for a linear chain are $R_g \sim M^{0.588}$ in a good solvent and $R_g \sim M^{0.5}$ in a Θ solvent. As the aqueous salt solution behaves as a good solvent for the polymer,[90−93] the difference between the results and theoretical relationship is most easily understood as branching in the molecules. Also shown in the Supporting Information is the GPC/MALS trace for the high-M dextran that was selected as matrix; its radius scales weakly with mass, $R_g \sim M^{0.13}$, suggesting that the molecules contain so many branching points that mass can be added without significantly increasing the molecular size. (This behavior cannot continue indefinitely; the inverse relation over the measured range, $M \sim R_g^8$ must give way to a solidlike $M \sim R_g^3$ at higher M values, if indeed such molecules exist.) Another possibility is that these large polymers were poorly separated.[48]

Turning to the rheology, in the measured range of oscillation frequency (1−100 Hz), no plateau was evident to signal an entangled system.[94] Ioan et al. did observe a storage modulus plateau at still lower frequencies; even so, the storage modulus was exceeded by the loss modulus over most of the frequency range. In our measurements, the storage modulus decreased slightly with concentration at every measured frequency, as illustrated in Figure 6. This may again be a consequence of branching. As the matrix polymers come closer together, yet remain unable to intertwine due to enhanced density at their cores, they may deswell due to a crowding effect.

SAXS scattering profiles are displayed in Figure 7. At the lowest concentration measured, the correlation length, ξ, between segments can be obtained cleanly from the Guinier relation, $I \propto \exp(-q^2\xi^2)$. At higher matrix concentrations, a peak emerges in the scattering profiles at some value q_{max}. This

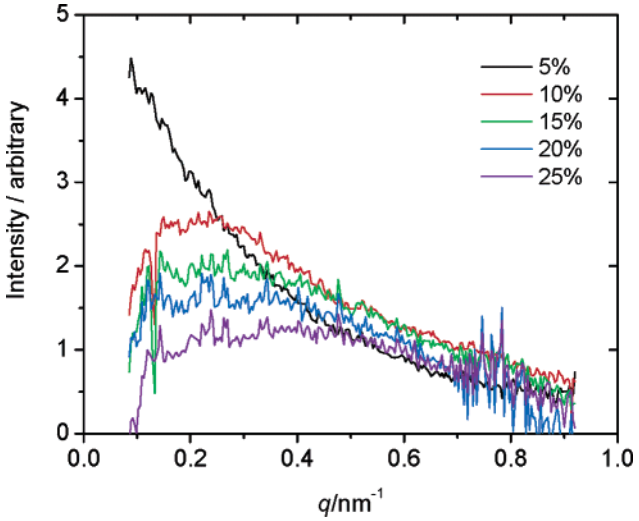

Figure 7. Overlay of scattering from dextran matrices in 5 mM NaN_3. From top to bottom (at $q = 0.2$ nm^{-1}) 0.05, 0.10, 0.15, 0.20, and 0.25.

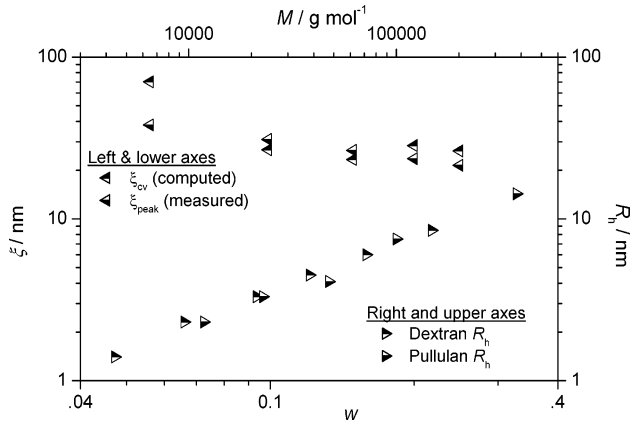

Figure 8. Comparison of dextran matrices ξ_{cv} and ξ_{peak}, with hydrodynamic radius (R_h) of the dextran and pullulan probes. ξ_{cv} is calculated using a matrix molecular weight of 2×10^6 g mol^{-1}, and R_h is calculated from D^0 measured with fluorescence photobleaching recovery.

suggests a characteristic distance, possibly intermolecular, denoted $\xi_{peak} = 2\pi/q_{max}$. Densely packed, branched molecules may act somewhat like spheres in solution. The average center-to-center distance at a given volume fraction, ξ_{CV}, is easily calculated. Figure 8 shows ξ_{peak} and ξ_{CV} as a function of weight fraction. The similarity between them leads to the conclusion that the peak in the scattering profile measures a characteristic distance between the matrix molecules in solution. For convenience, the hydrodynamic radius, R_h, of each dextran or pullulan is plotted on an ordinate of the same scale, choosing molecular weight as the abscissa. These R_h values were measured by FPR in dilute solutions and exceed the size of the diffuser when dispersed in the matrix. Even so, the probes are smaller than ξ_{peak} or ξ_{CV}, suggesting limited potential for interaction with the matrix molecules.

Combining the SAXS, rheology, and diffusion data, the matrix polymers appear to screen hydrodynamic interactions effectively, but they are not entangled.

Comparison of Diffusion Results to Selected Theoretical Treatments. Langevin and Rondelez[64,95] proposed a simple stretched exponential, eq 6, to describe the diffusion of probes in semidilute solutions or gel. In their model the diffusion normalized by its value in dilute solution absent any matrix, D/D^0, minus the quotient of viscosities η_0/η, depends on probe

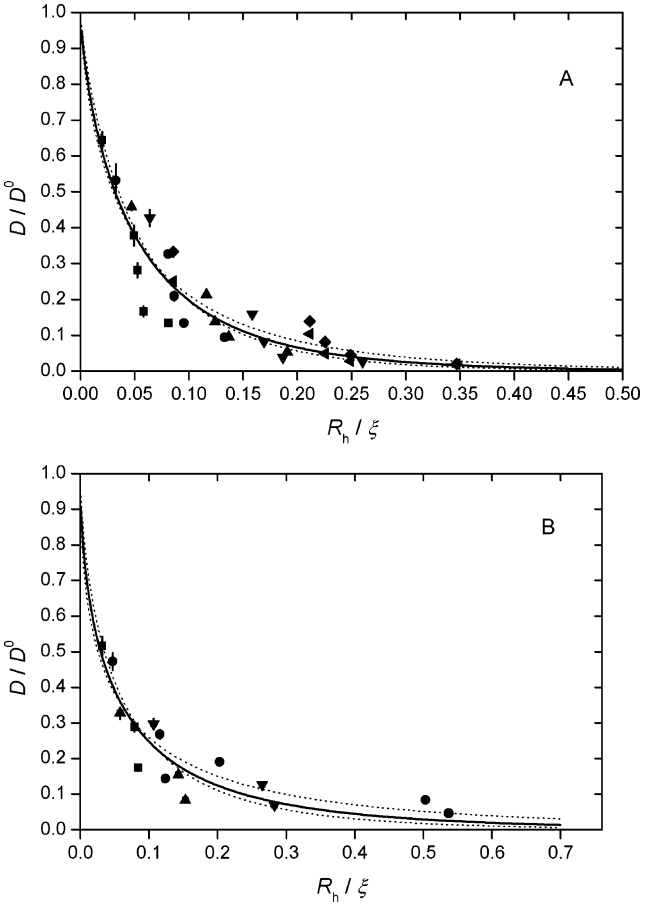

Figure 9. Langevin−Rondelez analysis of (A) labeled dextran and (B) labeled pullulan diffusing through dextran matrix solutions: (A) FD4 (squares); FD10s (circles); FD20 (up triangle); FD40 (down triangle); FD70 (diamond); FD150 (left-pointing triangle). (B) LP11.8 (squares); LP22.8 (circles); LP47.3 (up triangle); LP100 (down triangle); LP380 (left triangle).

radius and the correlation length of the matrix. Phillies and Streletzky revisited the idea of microrheology in polymer solutions using probe diffusers.[96] They proposed

$$D/D^0 = \exp[-\alpha'(R/\xi)^{\delta}] \tag{6}$$

Here, D is the diffusion of a spherical probe of radius R through the solution, D^0 is the diffusion of the probe absent any retarding matrix, and ξ is the correlation length of the matrix. The parameter δ (not to be confused with the same symbol in eq 5) is expected to be 2.5 for rigid gel matrices and should be less in solutions. The parameter α' can be adjusted to obtain the best fit. Included in α' are the solution properties of the mixtures. Data collected in this study include D, D^0, ξ, and R_h, allowing a master curve to be constructed if it is assumed that $R = R_h$, as calculated from D^0 using the Stokes−Einstein equation with a temperature of 298 K. Using a nonlinear least-squares analysis to fit eq 6 (Microcal Origin 6.1), it is found that $\delta = 0.744 \pm 0.074$ for labeled dextran diffusing through the matrix dextran solutions (Figure 9A). Russo and Bu measured an average δ of 0.63 for labeled dextran diffusing in solutions of HPC. The fit of the Langevin−Rondelez model to labeled pullulan diffusing through the dextran matrix solutions is shown in Figure 9B with $\delta = 0.577 \pm 0.086$.

An obstruction-scaling theory has been proposed by Amsden.[59,97] The model is intended for globular solutes, not branched probes as measured here, but it has the appealing characteristic that the molecular nature of the solution components is

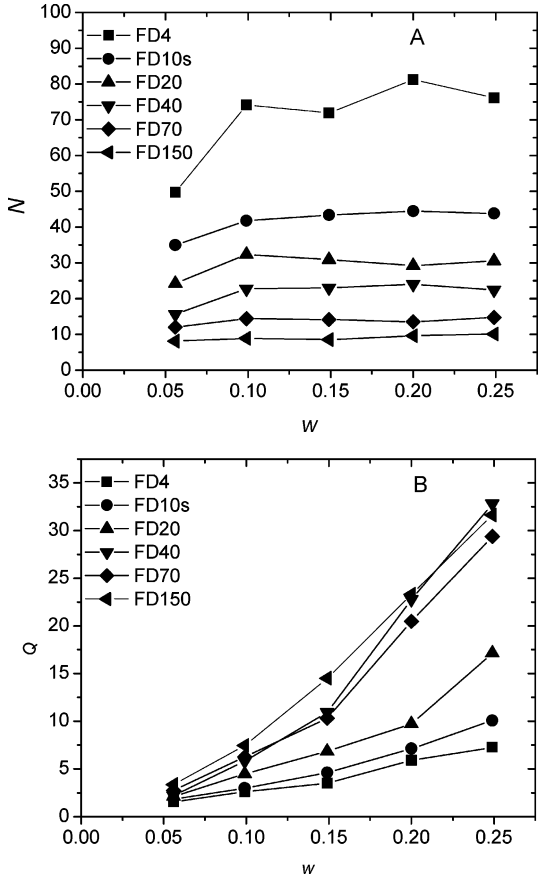

Figure 10. Analysis based on eq 2: (A) solved for N with parameter $Q = 1$; (B) solved for Q with parameter $N = 1$.

considered. The restraining polymer is modeled as a fiber, whose radius is estimated from chemical parameters. The model predicts that the probe diffusion declines according to

$$\frac{D}{D^0} = \frac{1}{Q}\exp\left[-\pi N\left(\frac{R+R_f}{\xi+2R_f}\right)^2\right] \tag{7}$$

where R_f is the fiber radius of the matrix polymer chain. In comparing to eq 6, the most significant difference is the exponent 2 in the argument to the transcendental term. Amsden computes $R_f = 0.692$ nm for dextran. The parameters Q and N do not appear in ref 59. They have been introduced because eq 7 predicts declines in diffusion that are far too modest compared to our data if used at $Q = N = 1$. The basis for eq 7 is

$$\frac{D}{D^0} = \frac{1}{Q}\int_{Nr^*}^{\infty} g(r)\,dr \tag{8}$$

where $g(r)$ is the distribution of radii between matrix fibers and r^* is the minimum radius for passage of the solute ($r^* = R + R_f$). From this form, it is evident that the introduction of parameter N implies that the chain will only pass larger openings of the fibers, while the parameter $Q \geq 1$ is introduced to express that a solute may not take advantage of every opening that is available. In this study, all parameters in eq 7 are known except N and Q. Either of these may depend on matrix concentration and probe molecular weight, so there are two variables and one equation for each probe−matrix combination. To gain some insight, we may set $Q = 1$ and solve for N. As shown in Figure 10A, N (at $Q = 1$) rises with matrix concentration and falls with probe molecular weight: if every opening in the matrix of fibers is diffusion-effective (i.e., $Q = 1$), then, within the

confines of the Amsden model applied to these data, pores in the fiber matrix must be larger than expected, the more so at low probe sizes and high matrix concentrations. This is difficult to explain. Conversely, if $N = 1$ (i.e, the required pore size is as expected), then Q rises with weight fraction of matrix polymer and overall with probe molecular weight, as shown in Figure 10B. It is not difficult to understand that more attempts to pass a barrier would be needed, the larger the probe and the more concentrated the matrix.

Conclusion

A problem that has long plagued studies of diffusion in complex media, namely that polydispersity of the probes becomes highly visible, can be viewed as an opportunity in macromolecular characterization. While trying to develop that potential, new physical features of dextran concentrated solutions have been identified. The systems studied do not approach the reptation limit, probably due to branching in the matrix polymer, yet the ability to resolve closely spaced components in a bimodal distribution is enhanced relative to free diffusion and can at least equal that available from GPC as normally practiced. Simulations suggest that performance will be very good at $\beta = 2$. These results should apply to other diffusion methods whenever the analyte and matrix signals are easily differentiated. Finally, there are reasons besides polydispersity why a population of molecules may not diffuse at identical rates. The quantification of the number of long chain branches comes to mind. In this regard, the good amplitude accuracy that was observed is very encouraging.

Acknowledgment. This material is based upon work supported by Dow Chemical and the National Science Foundation under Grant DMR-0075810. Garrett J. Doucet also acknowledges partial support through an NSF-IGERT fellowship (DGE-9987603), and David Neau acknowledges the support of an REU internship (CHE-9732195). We thank Dr. Wieslaw Stryjewski for the software development.

Supporting Information Available: Details of the data simulations, signal characteristics, GPC/MALS, and rheological measurements. This material is available free of charge via the Internet at http://pubs.acs.org.

References and Notes

(1) Moore, J. C. *J. Polym. Sci., Part B* **1964**, *2*, 835−843.
(2) Moore, J. C.; Hendrickson, J. G. *J. Polym. Sci., Part C: Polym. Symp.* **1965**, *No. 8*, 233−241.
(3) Moore, J. C. *J. Polym. Sci., Part A: Polym. Chem.* **1996**, *34*, 1833−1842.
(4) Porath, J.; Flodin, P. *Protides Biol. Fluids, Proc. Colloq.* **1963**, *10* 290−297.
(5) Lea, D. J.; Sehon, A. H. *Can. J. Chem.* **1962**, *40*, 159.
(6) Cortis-Jones, B. *Nature (London)* **1961**, *191*, 272−273.
(7) Vaughan, M. F. *Nature (London)* **1960**, *188*, 55.
(8) Porath, J.; Flodin, P. *Nature (London)* **1959**, *183*, 1657−1659.
(9) Lathe, G. H.; Ruthven, C. R. J., Jr. *Biochem. J.* **1956**, *62*, 665−674.
(10) Grubisic, Z.; Rempp, P.; Benoit, H. *J. Polym. Sci., Polym. Lett. Ed.* **1967**, *5*, 753−759.
(11) Benoit, H. *J. Polym. Sci., Polym. Phys. Ed.* **1996**, *34*, 1703−1704.
(12) Styring, M. G.; Armonas, J. E.; Hamielec, A. E. *J. Liq. Chromatogr.* **1987**, *10*, 783−804.
(13) Ouano, A. C. *J. Colloid Interface Sci.* **1978**, *63*, 275−281.
(14) Reed, W. F. *ACS Symp. Ser.* **2005**, *893*, 13−51.
(15) Provencher, S. W. *Comput. Phys.* **1982**, *27*, 213−227.
(16) Provencher, S. W. *Comput. Phys.* **1982**, *27*, 229−242.
(17) Chu, B.; Ying, O. C.; Wu, C.; Ford, J. R.; Dhadwal, H.; Qian, R. Y.; Bao, J. S.; Zhang, J. Y.; Xu, C. C. *Polym. Commun.* **1984**, *25*, 211−213.
(18) Chu, B.; Wu, C.; Zuo, J. *Macromolecules* **1987**, *20*, 700−702.
(19) Stepanek, P. Data analysis in dynamic light scattering. In *Dynamic Light Scattering, The Method and Some Applications*; Brown, W., Ed.; Clarendon Press: Oxford, 1993; Vol. 49, Chapter 4, pp 175−241.
(20) deGennes, P. G. *Scaling Concepts in Polymer Physics*; Cornell University Press: Ithaca, NY, 1979.
(21) Lodge, T. P. *Phys. Rev. Lett.* **1999**, *83*, 3218−3221.
(22) Chang, T.; Han, C. C.; Wheeler, L. M.; Lodge, T. P. *Macromolecules* **1988**, *21*, 1870−1872.
(23) Chu, B.; Wu, D.-Q. *Macromolecules* **1987**, *20*, 1606−1619.
(24) Lin, T.-H.; Phillies, G. D. J. *Macromolecules* **1984**, *17*, 1686−1691.
(25) Lodge, T. P. *Macromolecules* **1983**, *16*, 1393−1395.
(26) Phillies, G. D. J.; Streletzky, K. A. *Recent Research Developments in Physical Chemistry* **2001**, *5*, 269−285.
(27) Ullmann, G. S.; Ullmann, K.; Lindner, R. M.; Phillies, G. D. J. *J. Phys. Chem.* **1985**, *89*, 692−700.
(28) Martin, J. E. *Macromolecules* **1984**, *17*, 1279−1283.
(29) Lodge, T. P.; Wheeler, L. M.; Hanley, B.; Tirrell, M. *Polym. Bull. (Berlin)* **1986**, *15*, 35−41.
(30) Phillies, G. D. J. *J. Chem. Phys.* **1974**, *60*, 983−989.
(31) Akcasu, A. Z.; Nagele, G.; Klein, R. *Macromolecules* **1991**, *24*, 4408−4422.
(32) Lanni, F.; Ware, B. R. *Rev. Sci. Instrum.* **1982**, *53*, 905−908.
(33) Ware, B. R. *Am. Lab.* **1984**, *16*, 16−28.
(34) Axelrod, D.; Koppel, D. E.; Schlessinger, J.; Elson, E. L.; Webb, W. W. *Biophys. J.* **1976**, *16*, 1055−1066.
(35) Cong, R.; Turksen, S.; Russo, P. S. *Macromolecules* **2004**, *37*, 4731−4735.
(36) Kovaleski, J. M.; Wirth, M. J. *Anal. Chem.* **1997**, *69*, 600A−605A.
(37) Langevin, D. *Ber. Bunsen-Ges.* **1996**, *100*, 336−343.
(38) McNally, J. G.; Smith, C. L. *Confocal Two-Photon Microsc.* **2002**, 525−538.
(39) Meyvis, T. K. L.; De Smedt, S. C.; Van Oostveldt, P.; Demeester, J. *Pharm. Res.* **1999**, *16*, 1153−1162.
(40) Robinson, J. P. *Methods Cell Biol.* **2001**, *63*, 89−106.
(41) Verkman, A. S. *Methods Enzymol.* **2003**, *360*, 635−648.
(42) Russo, P. S.; Qiu, J.; Edwin, N.; Choi, Y.-W.; Doucet, G.; Sohn, D. Fluorescence Photobleaching Recovery, a Primer. In *Soft Matter: Scattering, Imaging and Manipulation*; Pecora, R., Borsali, R., Eds.; Springer: New York; in press.
(43) Cicerone, M. T.; Blackburn, F. R.; Ediger, M. D. *Macromolecules* **1995**, *28*, 8225−8232.
(44) Davoust, J.; Devaux, P. F.; Leger, L. *EMBO J.* **1982**, *1*, 1233−1238.
(45) Smith, B. A.; McConnell, H. M. *Proc. Natl. Acad. Sci. U.S.A.* **1978**, *75* 2759−2763.
(46) Fong, B.; Stryjewski, W.; Russo, P. S. *J. Colloid Interface Sci.* **2001**, *239*, 374−379.
(47) Chu, B. *Laser Light Scattering*, 2nd ed.; Academic Press: New York, 1991.
(48) Ioan, C. E.; Aberle, T.; Burchard, W. *Macromolecules* **2000**, *33*, 5730−5739.
(49) Furukawa, R.; Arauz-Lara, J. L.; Ware, B. R. *Macromolecules* **1991**, *24*, 599−605.
(50) Granath, K. A. *J. Colloid Sci.* **1958**, *13*, 308−328.
(51) Ioan, C. E.; Aberle, T.; Burchard, W. *Macromolecules* **2001**, *34*, 326−336.
(52) Nordmeier, E.; Xing, H.; Lechner, M. D. *Makromol. Chem., Macromol. Chem. Phys.* **1993**, *194*, 2923−2937.
(53) Nordmeier, E. *J. Phys. Chem.* **1993**, *97*, 5770−5785.
(54) Wu, C. *Macromolecules* **1993**, *26*, 3821−3825.
(55) Zhou, R. *Zhongguo Yaoxue Zazhi* **1992**, *27*, 159−162.
(56) Luby-Phelps, K.; Castle, P. E.; Taylor, D. L.; Lanni, F. *Proc. Natl. Acad. Sci. U.S.A.* **1987**, *84*, 4910−4913.
(57) Kwak, S.; Lafleur, M. *Macromolecules* **2003**, *36*, 3189−3195.
(58) Kosar, T. F.; Phillips, R. J. *AIChE J.* **1995**, *41*, 701−711.
(59) Amsden, B. *Polymer* **2002**, *43*, 1623−1630.
(60) Ogston, A. G. *Trans. Faraday Soc.* **1958**, *54*, 1754−1757.
(61) Ogston, A. G.; Preston, B. N.; Wells, J. D.; Snowden, J. M. *Proc. R. Soc. London, Ser. A* **1973**, *333*, 297−316.
(62) Muhr, A. H.; Blanshard, J. M. V. *Polymer* **1982**, *23* (July), 1012−1026.
(63) Cukier, R. I. *Macromolecules* **1984**, *17*, 252−255.
(64) Langevin, D.; Rondelez, F. *Polymer* **1978**, *19*, 875−882.
(65) Phillies, G. D. J. *Macromolecules* **1998**, *31*, 2317−2327.
(66) Altenberger, A. R.; Dahler, J. S.; Tirrell, M. *Macromolecules* **1988**, *21*, 464−469.
(67) Altenberger, A. R.; Tirrell, M. *J. Chem. Phys.* **1984**, *80* 2208−2213.
(68) Johansson, L.; Elvingson, C.; Lofroth, J. E. *Macromolecules* **1991**, *24*, 6024−6029.
(69) Johnson, E. M.; Berk, D. A.; Jain, R. K.; Deen, W. M. *Biophys. J.* **1996**, *70*, 1017−1026.
(70) Cheng, Y.; Prud'homme, R. K.; Thomas, J. *Macromolecules* **2002**, *35*, 8111−8121.

(71) Ostrowsky, N.; Sornette, D.; Parker, P.; Pike, E. R. *Opt. Acta* **1981**, *28*, 1059−1070.
(72) Bertero, M.; Brianzi, P.; Pike, E. R.; de Villiers, G.; Lan, K. H.; Ostrowsky, N. *J. Chem. Phys.* **1985**, *82*, 1551−1554.
(73) McWhirter, J. G. *Opt. Acta* **1980**, *27*, 83−105.
(74) McWhirter, J. G.; Pike, E. R. *J. Phys. A: Math. Gen.* **1978**, *11*, 1729−1745.
(75) Boyd, W. C. *J. Biol. Chem.* **1965**, *240*, 4097−4098.
(76) Bu, Z.; Russo, P. S. *Macromolecules* **1994**, *27*, 1187−1194.
(77) Yamakawa, H. *Modern Theory of Polymer Solutions*; Harper and Row: New York, 1971.
(78) Tirrell, M. *Rubber Chem. Technol.* **1984**, *57*, 523−556.
(79) Lodge, T. P. *Phys. Rev. Lett.* **1999**, *83*, 3218−3221.
(80) Lodge, T. P. *Macromolecules* **1993**, *16*, 1393−1395.
(81) Wheeler, L. M.; Lodge, T. P. *Macromolecules* **1989**, *22*, 3399−3408.
(82) Wang, S. F.; Wang, S. Q.; Halasa, A.; Hsu, W. L. *Macromolecules* **2003**, *36*, 5355−5371.
(83) Doucet, G. Ph.D. Dissertation Louisiana State University, 2004.
(84) Chang, T.; Han, C. C.; Wheeler, L.; Lodge, T. P. *Macromolecules* **1988**, *21*, 1870−1872.
(85) Furukawa, R.; Arauz-Lara, J. L.; Ware, B. R. *Macromolecules* **1991**, *24*, 599−605.
(86) Gohr, K.; Schartl, W. *Macromolecules* **2000**, *33*, 2129−2135.
(87) Ioan, C. E.; Aberle, T.; Burchard, W. *Macromolecules* **1999**, *32*, 8655−8662.
(88) Galinsky, G.; Burchard, W. *Macromolecules* **1996**, *29*, 1498−1506.
(89) Graessley, W. W.; Edwards, S. F. *Polymer* **1981**, *22*, 1329−1334.
(90) Barker, P. E.; England, K.; Ganetsos, G. *J. Chem. Technol. Biotechnol.* **1988**, *41*, 61−68.
(91) Cooper, A. R.; Matzinger, D. P. *J. Liq. Chromatogr.* **1978**, *1*, 745−759.
(92) Desbrieres, J.; Mazet, J.; Rinaudo, M. *Eur. Polym. J.* **1982**, *18*, 269−272.
(93) Granath, K. A.; Flodin, P. G. M. *Makromol. Chem.* **1961**, *48*, 160−171.
(94) Doi, M.; Edwards, S. F. *The Theory of Polymer Dynamics*; Oxford University Press: Oxford, 1998.
(95) Langevin, D. *Polymer* **1978**, *19*, 875−882.
(96) Phillies, G. D. J.; Streletzky, K. A. *Recent Res. Dev. Phys. Chem.* **2001**, *5*, 269−285.
(97) Amsden, B. *Macromolecules* **1999**, *32*, 874−879.

MA0608525